

Communication

Second-Order Statistics of Self-Splitting Structured Beams in Oceanic Turbulence

Liming Liu ^{1,2}, Yulu Liu ¹, Hao Chang ^{1,2}, Jifei Huang ^{1,2}, Xinlei Zhu ^{1,2}, Yangjian Cai ^{1,2,*} and Jiayi Yu ^{1,2,*} 

¹ Shandong Provincial Key Laboratory of Optics and Photonic Devices, Shandong Provincial Engineering and Technical Center of Light Manipulation, School of Physics and Electronics, Shandong Normal University, Jinan 250358, China

² Collaborative Innovation Center of Light Manipulation and Applications, Shandong Normal University, Jinan 250358, China

* Correspondence: yangjiancai@sdu.edu.cn (Y.C.); jiayiyu0528@sdu.edu.cn (J.Y.)

Abstract: Free-space optical communication is restricted by random media-stimulated beam degradation. However, partially coherent structured beams modulated by the coherence structure can potentially mitigate this negative effect. By employing the extended Huygens–Fresnel integral, we provide an examination of the second-order statistical features of a common type of partly coherent structured beams, self-splitting structured beams, in a turbulent ocean. The implications of turbulence parameters relating to the ocean and beginning beam parameters corresponding to the progression of such beam propagation attributes are fully investigated. Our numerical outcomes show that, for turbulence with a low-dissipation kinetic energy rate per unit mass of fluid, small Kolmogorov inner scale, large relative strength of temperature to salinity undulations, and large dissipation rate of mean-square temperature has a greater negative effect on the structured beams. In addition, we suggest an effective approach, enhancing the order of the beam and reducing the coherence length of the beams, to lower the oceanic turbulence-induced negative effects, and thus have future extensive possibilities in free-space optical communication.

Keywords: partially coherent structured beam; oceanic turbulence; propagation



Citation: Liu, L.; Liu, Y.; Chang, H.; Huang, J.; Zhu, X.; Cai, Y.; Yu, J. Second-Order Statistics of Self-Splitting Structured Beams in Oceanic Turbulence. *Photonics* **2023**, *10*, 339. <https://doi.org/10.3390/photonics10030339>

Received: 27 February 2023

Revised: 14 March 2023

Accepted: 19 March 2023

Published: 22 March 2023



Copyright: © 2023 by the authors. Licensee MDPI, Basel, Switzerland. This article is an open access article distributed under the terms and conditions of the Creative Commons Attribution (CC BY) license (<https://creativecommons.org/licenses/by/4.0/>).

1. Introduction

One of the most important laser uses is free-space optical (FSO) communication, which utilizes the wireless transmission of data to receivers via light beam propagations. The environment where the light beam is located is not a perfect vacuum; it will be affected by random media, causing beam quality degradation, and limiting the development of FSO communication [1]. As a result, in recent decades, there has been a great deal of interest in studying beams of light and their propagation characteristics in random media and developing techniques to mitigate the deleterious impacts of random media on light beams [2–4].

A generally understood fact is that altering beam coherence is a useful method for improving light beam performance in random media [3,5]. Numerous studies have shown that partially coherent structured beams, whose spatial coherence has been reduced [6], have smaller turbulence-stimulated negative effects compared to their completely coherent counterparts [7–13]. Shirai et al. presented a scientific interpretation for this resistance using the coherent mode representation, implying that a light beam is delivered across many non-interfering channels at the same time [14]. With the development of modulation technology of the coherence structure of light beams [15], more light beams with specific coherence structures are tailored [16]. Such beams display unusual propagation features caused by prescribed coherence structure, examples include self-focusing and lateral shifting of the intensity maximum, far-field beam profile shaping, self-splitting, furthermore, such beams

also possess better resistance to random media [8–10,17–20], and it is also a strategy for encoding information into the coherence structure to transmission [21,22].

Coherence manipulation of light beams brings vitality to studies on the propagation of electromagnetic radiation in random media. However, scholars have previously preferred to study the propagation attributes of electromagnetic beams within a turbulent atmosphere and thereby often overlook the turbulent ocean that encompasses 71% of the total area of the planet. This pattern could be explained by the fact that the spectra of refractive index (relating to power) changes in both the ocean and atmosphere to a similar extent and involve a comparable system [1,23]. The authors are aware that refraction is the primary cause of light beam disturbance in the water, other than absorption and scattering [4,23], and the primary drivers of turbulence in the ocean are fluctuations in humidity, salinity, temperature, and irregular movement of water. Light beam propagation in a turbulent ocean is more complicated than that in a turbulent atmosphere. Therefore, as underwater technologies advance, it is important and vital to examine how oceanic turbulence has an effect on the characteristics of light beams as they propagate and to look for a solution to lessen the impact that oceanic turbulence has on beams of light. In 2019, it was addressed how a rotating elliptical Gaussian optical coherence lattice propagated in oceanic turbulence. Such findings demonstrated that every sub-beam in such a lattice retains a regulated rotation within a specific distance; this is crucial for alleviating turbulence effects [24]. Recently, the effect of the parameters for the oceanic turbulence on multi-sinc Schell-model beams was explored explicitly [25]. The best we can tell, though, is that there are many reports on the oceanic turbulence effects on partially coherent structured beams, but few of them discuss in detail the impact of the coherence structure parameters of beams on turbulence resistance.

In this paper, we choose a self-splitting structured (SSS) beam as the research object and focus on discussing its propagation properties in the presence of oceanic turbulence, and the consequences of the parameters of this type of turbulence on the second-order statistical characteristics of such beams. Additionally, we offer a method for modifying the coherence length, the beam order, and the starting beam parameters in order to preserve the self-splitting propagation features and lessen the detrimental impacts brought on by ocean turbulence. In Section 2, the analytical expressions of the cross-spectral density of SSS beams in a turbulent ocean are derived based on the extended Huygens–Fresnel principle. In Section 3, the analytical expressions of propagation factor and relative radius of curvature of SSS beams in turbulence are derived based on the Wigner distribution function. In Section 4, the numerical calculation and results are presented and discussed. In Section 5, the conclusion and observation are presented.

2. Cross-Spectral Density of SSS Beams in Oceanic Turbulence

The cross-spectral density of the SSS beam at the source plane ($z = 0$) is written as [26]

$$W_0(\mathbf{r}_1, \mathbf{r}_2) = \tau^*(\mathbf{r}_1)\tau(\mathbf{r}_2)\mu(\mathbf{r}_1, \mathbf{r}_2), \tag{1}$$

in which $\mathbf{r}_1 = (x_1, y_1)$ and $\mathbf{r}_2 = (x_2, y_2)$ represent the two transverse position vectors in the source plane. Here, the asterisk signifies a complex conjugate and the amplitude function $\tau(\mathbf{r}) = \exp(-\mathbf{r}^2/w^2)$ with w as the beam width. Moreover, $\mu(\mathbf{r}_1, \mathbf{r}_2)$ represents the spectral degree of coherence (SDOC), which is explicitly written as

$$\mu(\mathbf{r}_1 - \mathbf{r}_2) = \prod_{\zeta=x,y} \left[G_0 H_{2m} \left(\frac{\zeta_1 - \zeta_2}{\sqrt{2}\delta_\zeta} \right) \exp \left(-\frac{(\zeta_1 - \zeta_2)^2}{2\delta_\zeta^2} \right) \right], \tag{2}$$

where \prod represents a product over a set of terms denoted by $\zeta = x, y$, a constant $G_0 = 1/H_{2m}(0)$, which incorporates H_{2m} and signifies the Hermite polynomial of order $2m$, and δ_ζ denotes the spatial coherence length along the ζ -direction.

With respect to the paraxial approximation, a partly coherent structured beam propagating along the positive half plane (i.e., $z > 0$) in a random medium requires the employment of the generalized Huygens–Fresnel integral [1]

$$W(\boldsymbol{\rho}_1, \boldsymbol{\rho}_2, z) = \frac{1}{\lambda^2 z^2} \iint_{-\infty}^{+\infty} W_0(\mathbf{r}_1, \mathbf{r}_2) \exp\left\{-\frac{ik}{2z} [(\boldsymbol{\rho}_1 - \mathbf{r}_1)^2 - (\boldsymbol{\rho}_2 - \mathbf{r}_2)^2]\right\} \times \langle \exp[\Psi^*(\mathbf{r}_1, \boldsymbol{\rho}_1, z) + \Psi(\mathbf{r}_2, \boldsymbol{\rho}_2, z)] \rangle d^2\mathbf{r}_1 d^2\mathbf{r}_2, \tag{3}$$

where $k = 2\pi/\lambda$ is the wave number, in which λ is the wavelength, and $\boldsymbol{\rho}_1 = (\rho_{1x}, \rho_{1y})$ and $\boldsymbol{\rho}_2 = (\rho_{2x}, \rho_{2y})$ are two spatial positions in the target plane. The random transmission medium’s fluctuating refractive index between the source and destination planes results in a complex perturbation phase called $\Psi(\mathbf{r}, \boldsymbol{\rho}, z)$. $\langle \ \rangle$ denotes ensemble average, and the following formula can be used to express the ensemble average term [1]

$$\langle \exp[\Psi^*(\mathbf{r}_1, \boldsymbol{\rho}_1, z) + \Psi(\mathbf{r}_2, \boldsymbol{\rho}_2, z)] \rangle = \exp\left\{-4\pi^2 k^2 z \int_0^1 d\psi \int_0^\infty \kappa \Phi(\kappa) d^2\kappa [1 - J_0[\kappa|\psi(\mathbf{r}_1 - \mathbf{r}_2) + (1 - \psi)(\boldsymbol{\rho}_1 - \boldsymbol{\rho}_2)|]]\right\}, \tag{4}$$

with J_0 is the zero-order Bessel function, which can be approximated as

$$J_0[\kappa|\psi(\mathbf{r}_1 - \mathbf{r}_2) + (1 - \psi)(\boldsymbol{\rho}_1 - \boldsymbol{\rho}_2)|] \sim 1 - \frac{1}{4} [(1 - \psi)(\boldsymbol{\rho}_1 - \boldsymbol{\rho}_2) + \psi(\mathbf{r}_1 - \mathbf{r}_2)]^2 \kappa^2. \tag{5}$$

Substituting the relation Equation (5) into Equation (4), one acquires the ensemble average term in Equation (3) as

$$\langle \exp[\Psi^*(\mathbf{r}_1, \boldsymbol{\rho}_1, z) + \Psi(\mathbf{r}_2, \boldsymbol{\rho}_2, z)] \rangle = \exp\left\{-k\Omega T z^{-1} [(\boldsymbol{\rho}_1 - \boldsymbol{\rho}_2)^2 + (\boldsymbol{\rho}_1 - \boldsymbol{\rho}_2) \cdot (\mathbf{r}_1 - \mathbf{r}_2) + (\mathbf{r}_1 - \mathbf{r}_2)^2]\right\}, \tag{6}$$

where $\Omega = k\pi^2 z^2/3$, $T = \int_0^\infty \kappa^3 \Phi(\kappa) d^2\kappa$, in which $\Phi(\kappa)$ signifies the spectrum (relating to power) of the refractive fluctuations due to oceanic turbulent. The latter is defined as [8,27]

$$\Phi(\kappa) = C_0 \varepsilon^{-1/3} \kappa^{-11/3} \chi_T \left[1 + 2.35(\kappa\eta)^{2/3}\right] \times \left[\exp(-A_T\sigma) + \frac{\exp(-A_S\sigma)}{\omega^2} - \frac{2\exp(-A_{TS}\sigma)}{\omega}\right], \tag{7}$$

where $C_0 = 0.388 \times 10^{-8}$. Moreover, ε is the dissipation kinetic energy rate per unit mass of fluid, which has a value between $10^{-1} \text{m}^2/\text{s}^3$ and $10^{-10} \text{m}^2/\text{s}^3$. And χ_T is the dissipation rate of mean-square temperature (between $10^{-4} \text{K}^2/\text{s}$ and $10^{-10} \text{K}^2/\text{s}$). In addition, ω is the relative strength of temperature to salinity fluctuations, (from -5 to 0) and η is the Kolmogorov inner scale. The quantities used are $A_T = 1.863 \times 10^{-2}$, $A_S = 1.9 \times 10^{-4}$, $A_{TS} = 9.41 \times 10^{-3}$ and $\sigma = 8.284(\kappa\eta)^{4/3} + 12.978(\kappa\eta)^2$. Thus, it is possible to express T as [23]

$$T = C_0 \varepsilon^{-1/3} \chi_T \eta^{-1/3} (45.5708\omega^{-2} - 17.6701\omega^{-1} + 6.78335). \tag{8}$$

By inserting Equation (1) into Equation (3), which is followed by a rather tedious integration, the cross-spectral density of the SSS beams in the target plane is obtained

$$W(\boldsymbol{\rho}_1, \boldsymbol{\rho}_2, z) = \prod_{\xi=x,y} \left\{ \frac{G_0 P \delta_\xi}{a_\xi^{m+1/2}} (a_\xi - 1)^m H_{2m} \left[-\frac{b_\xi}{2\sqrt{a_\xi^2 - a_\xi}} \right] \times \exp \left[\frac{b_\xi^2}{4a_\xi} - \frac{iP}{w} \Re_{s\xi} \Re_{d\xi} - \left(\frac{2P}{w} \Omega T + \frac{P^2}{2} \right) \Re_{d\xi}^2 \right] \right\}, \tag{9}$$

with

$$\begin{aligned}
 a_{\xi} &= 2\delta_{\xi}^2 \left(\frac{1}{8w^2} + \frac{P\Omega T}{w} + \frac{1}{2\delta_{\xi}^2} + \frac{P^2}{2} \right); \\
 b_{\xi} &= \sqrt{2}\delta_{\xi} \left(\frac{iP}{w} \Re_{s\xi} + P^2 \Re_{d\xi} \right); \quad P = \frac{kw}{z}.
 \end{aligned}
 \tag{10}$$

To simplify the operation in the above integral, “sum” and “difference” coordinates are introduced, which are defined as

$$\begin{aligned}
 \mathbf{r}_s &= (\mathbf{r}_1 + \mathbf{r}_2)/2; \quad \mathbf{r}_d = \mathbf{r}_1 - \mathbf{r}_2; \\
 \Re_s &= (\Re_1 + \Re_2)/2; \quad \Re_d = \Re_1 - \Re_2,
 \end{aligned}
 \tag{11}$$

with

$$\Re_1 = \rho_1 + i\Omega T(\rho_1 - \rho_2); \quad \Re_2 = \rho_2 + i\Omega T(\rho_1 - \rho_2).
 \tag{12}$$

As a result, we can use Equation (9) to obtain the cross-spectral density of the SSS beams within the target plane and use the definition to examine the spectral strength of such beams, that is, [6]

$$S(\rho, z) = W(\rho, \rho, z).
 \tag{13}$$

The SDOC of such beams within the target plane is obtained from [6]

$$\mu(\rho_1, \rho_2, z) = \frac{W(\rho_1, \rho_2, z)}{\sqrt{W(\rho_1, \rho_1, z)W(\rho_2, \rho_2, z)}}.
 \tag{14}$$

3. Propagation Factors and Relative Radius of Curvature of SSS Beams in Oceanic Turbulence

Because the physics of partially coherent structured beams propagating in oceanic turbulence is complex, a number of different variables can be examined to determine how the turbulence affects partially coherent structured beams. Studying the beam’s global attributes, such as its relative radius of curvature and propagation factor, is the simplest strategy. These can all be estimated using the Wigner distribution function (WDF) and represented with respect to the second-order moments of the beams. Expressions for the relative radius of curvature and the propagation factor of such beams, under oceanic turbulence conditions, are then derived in this section. This occurs after the analytical formulations are first derived for the second-order moments of the WDF of the SSS beams under the effects of oceanic turbulence. The impact of turbulence on the propagation of the beam is well described by these global factors, which we shall explore in more detail in the next section. By using the following formula, the WDF of a partially coherent structured beam is expressible in terms of the cross-spectral density [28]

$$h(\rho_s, \theta, z) = \frac{1}{\lambda^2} \int_{-\infty}^{+\infty} W(\rho_s, \rho_d, z) \exp(-ik\theta \cdot \rho_d) d^2\rho_d,
 \tag{15}$$

where $\theta = (\theta_x, \theta_y)$ represents the angle of the relevant vector with respect to the z-direction, while $k\theta_x$ and $k\theta_y$ are the wave vector components aligning with the x-axis and y-axis, respectively. Using Equation (3), the term $W(\rho_s, \rho_d, z)$ is expressible in the alternative form that follows

$$\begin{aligned}
 W(\rho_s, \rho_d, z) &= \frac{1}{4\pi^2} \iiint_{-\infty}^{+\infty} W_0\left(\mathbf{r}_s, \rho_d + \frac{w}{P}\boldsymbol{\kappa}_d\right) d^2\mathbf{r}_s d^2\boldsymbol{\kappa}_d \\
 &\quad \times \exp\left[-i\rho_s \cdot \boldsymbol{\kappa}_d + i\mathbf{r}_s \cdot \boldsymbol{\kappa}_d - \Theta\left(\rho_d, \rho_d + \frac{w}{P}\boldsymbol{\kappa}_d\right)\right],
 \end{aligned}
 \tag{16}$$

with

$$\Theta\left(\rho_d, \rho_d + \frac{w}{P}\boldsymbol{\kappa}_d\right) = 3\Omega T \left(\frac{P}{w}\rho_d^2 + \rho_d \cdot \boldsymbol{\kappa} + \frac{w}{3P}\boldsymbol{\kappa}^2 \right),
 \tag{17}$$

where ρ_s and ρ_d also satisfy the “sum” and “difference” coordinate forms as shown in Equation (11).

Applying Equations (15)–(17), the following is how we arrive at the equation for the WDF of the SSS beams traversing into oceanic turbulence

$$h(\rho_s, \theta, z) = \prod_{\xi=x,y} h(\rho_{s\xi}, \theta_\xi, z), \tag{18}$$

where

$$h(\rho_{s\xi}, \theta_\xi, z) = \frac{G_0 w}{\lambda \sqrt{2\pi}} \int_{-\infty}^{+\infty} H_{2m} \left[-\frac{1}{\sqrt{2\delta_\xi}} \left(\rho_{d\xi} + \frac{w}{P} \kappa_{d\xi} \right) \right] \times \exp \left(-c_\xi \rho_{d\xi}^2 - d_\xi \kappa_{d\xi}^2 - e_\xi \rho_{d\xi} \kappa_{d\xi} - ik \theta_\xi \rho_{d\xi} \right) d\kappa_{d\xi} d\rho_{d\xi}, \tag{19}$$

with

$$c_\xi = \frac{1}{2\delta_\xi^2} + \frac{1}{8w^2} + \frac{3P\Omega T}{w}; \quad d_\xi = \frac{w^2}{2\delta_\xi^2 P^2} + \frac{1}{8P^2} + \frac{w^2}{2} + \frac{3w\Omega T}{P}; \tag{20}$$

$$e_\xi = \frac{w}{\delta_\xi^2 P} + \frac{1}{4wP} + 3\Omega T.$$

The orderly moments $n_1 + n_2 + m_1 + m_2$ of the WDF of a beam consists of [28]

$$\langle x^{n_1} y^{n_2} \theta_x^{m_1} \theta_y^{m_2} \rangle = \frac{1}{\Lambda} \iiint \int_{-\infty}^{+\infty} x^{n_1} y^{n_2} \theta_x^{m_1} \theta_y^{m_2} h(\rho_s, \theta, z) d^2 \rho_s d^2 \theta, \tag{21}$$

where

$$\Lambda = \iiint \int_{-\infty}^{+\infty} h(\rho_s, \theta, z) d^2 \rho_s d^2 \theta. \tag{22}$$

Then, substituting Equation (19) into Equation (21), one obtains the second-order moments of WDF of the SSS beams traversing through oceanic turbulence, that is,

$$\langle \rho_\xi^2 \rangle = -\frac{2mz^2}{k^2 \delta_\xi^2} - 2b_\xi; \quad \langle \theta_\xi^2 \rangle = -\frac{2m}{k^2 \delta_\xi^2} - \frac{2a_\xi}{k^2}; \quad \langle \rho_\xi \theta_\xi \rangle = -\frac{2mz}{k^2 \delta_\xi^2} - \frac{c_\xi}{k}. \tag{23}$$

The aforementioned second-order moments enable an assessment of the beam quality metric, which is expressed as [29]

$$Q = \langle \rho^2 \rangle \langle \theta^2 \rangle - \langle \rho \cdot \theta \rangle^2. \tag{24}$$

This variable correlates with the beam propagation factor $M^2 = \sqrt{Q}$. Taking a certain beam width at the source plane, lower beam divergence, and the correspondingly reduced M^2 are related to improved beam quality. Next, we consider the propagation factors that align with the x - and y -directions, due to the beam being rectangularly symmetric. Substituting Equations (23) into Equation (24), we obtain an explicit expression for the propagation factor of the SSS beams in the oceanic turbulence.

We can also study the curvature radius that align with the x - and y -directions of such beams in a turbulent ocean by considering the second-order moments of WDF, so that [30]

$$R_\xi = \frac{\langle \rho_\xi^2 \rangle}{\langle \rho_\xi \theta_\xi \rangle}. \tag{25}$$

In order to better conduct comparative studies, we define the relative radius of curvature

$$\Delta R_\xi = \frac{|R_{tur} - R_{free}|}{R_{free}}, \tag{26}$$

where R_{tur} and R_{free} represent the beam’s curvature radius in oceanic turbulence and in free space, respectively.

4. Numerical Calculation and Analysis of Second-Order Statistics of SSS Beams

The second-order statistics of SSS beams traversing through oceanic turbulence are examined using the expressions that were derived in earlier sections. In the examples that follow, unless stated otherwise, the initial settings for the turbulence and the beam parameters are given as follows: $\lambda = 632.8$ nm, $w = 1$ cm, $\delta_x = \delta_y = \delta = 5$ mm, $\varepsilon = 10^{-3}$ m²/s³, $\chi_T = 10^{-8}$ K²/s, $\eta = 1$ mm, and $\omega = -3.0$. For convenience, the wavelength is taken as that of a common HeNe-type laser diode; the results presented here are qualitatively similar for optical communication wavelengths.

Figure 1 depicts the evolution of an SSS beam’s SDOC modulus, at various propagation lengths, in oceanic turbulence and for free space. The diagrams within this figure demonstrate that the SDOC of the SSS beam is spread in an array at the source plane and, while the beam traverses across free space, the array distribution gradually vanishes before changing into a diamond distribution. However, in oceanic turbulence, the SDOC evolves into an array distribution in the short propagation distance, and then eventually develops in the far field into a Gaussian distribution. From which we can conclude that the SDOC of the SSS beam is degraded due to the negative effects caused by oceanic turbulence.

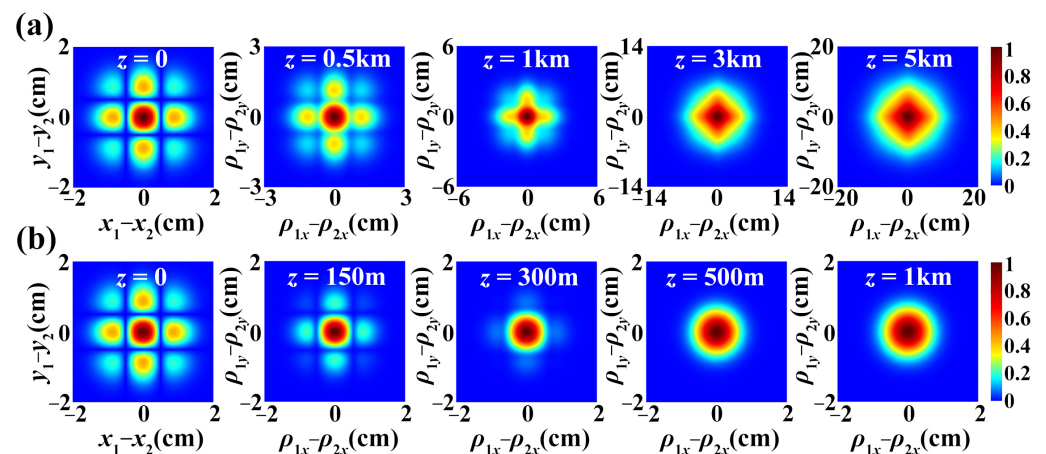


Figure 1. Evolution of the SDOC modulus of an SSS beam when traversing through (a) free space and (b) oceanic turbulence.

The evolution of the SSS beam propagating in free space, in terms of intensity, is shown in Figure 2a. It displays normalized density plots of the transverse spectral intensity for various propagation distances. As the propagation distance grows, it is clearly observable that four beam spots eventually develop from the original single beam spot while propagating, i.e., the SSS beam displays splitting characteristics as it travels. Figure 2b depicts how the spectral intensity changes over time in oceanic turbulence. The fact that such a beam still seems to exhibit splitting properties is shown when propagating over a short distance, while the intensity distribution of the spectra steadily develops into a Gaussian form over longer distances. This is due to the fact that, when the propagation distance is low, the beam’s free-space diffraction dominates, whereas the isotropic effect of oceanic turbulence progressively builds up and dominates as the propagation distance grows.

Following that, we will talk about how turbulence parameters affect the SDOC and spectrum intensity of the suggested beams and how the initial beam parameters help the beams resist the negative impacts of oceanic turbulence.

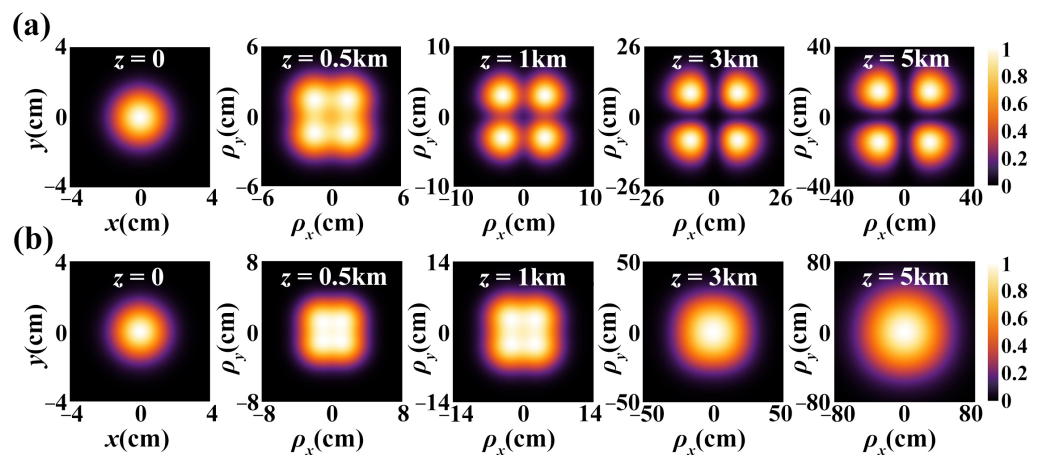


Figure 2. Development of the normalized spectral intensity of an SSS beam traversing through (a) free space and (b) oceanic turbulence.

Figure 3 illustrates the SDOC modulus of the SSS beam for a propagation distance of $z = 300$ m, while assuming various oceanic turbulence parameters. On the SDOC degradation in oceanic turbulence, the impacts of different dissipation rate values for the kinetic energy per unit mass of the fluid are compared in Figure 3a. The SDOC distribution in oceanic turbulence exhibits side lobes when the kinetic energy dissipation rate per unit mass of the fluid takes a high value, and it degenerates more quickly to a Gaussian form as the dissipation rate drops. Thus, it may be concluded that the development of the spectral degree of coherence of the SSS beam is significantly harmed by oceanic turbulence, which has a low kinetic energy dissipation rate per unit mass of the fluid. The slower degradation of SDOC can be attributed to reduced oceanic turbulence, which is caused by the faster dissipation rate of kinetic energy per unit mass of fluid. With a similar analysis, the following conclusions are drawn from Figure 3b–d. The oceanic turbulence containing a small Kolmogorov inner scale, alternatively with an extensive dissipation rate for the mean-square temperature or with a substantial relative strength for the temperature to salinity undulations, has a sizeable negative effect on the SSS beam from the perspective of the degeneration of the SDOC. It makes sense that the significant light scattering will be caused by the smaller inner scale of turbulence. As the light scattering increases, the degeneration of the SDOC caused by oceanic turbulence increases. The more energetic turbulence is often determined by the mean-squared temperature dissipation rate, which leads to enhanced SDOC degeneration. Regarding the case, the temperature and salinity undulations’ relative strength $\omega \rightarrow -5$, the temperature field’s volatility dominates. Whereas when $\omega \rightarrow 0$, the fluctuation of the salinity field is dominant. This suggests that the deterioration of the SDOC of the SSS beams is greatly influenced by the salinity fluctuations in comparison to the temperature fluctuations. Therefore, the SSS beams propagating in deep-sea regions can maintain the beam performance better in shallow-sea regions.

Our understanding of the impact of various turbulence characteristics on the propagation properties of the SSS beams in oceanic turbulence is based on the analysis provided earlier. Realistically, modifying the characteristics of oceanic turbulence is extremely difficult. Hence, we require an investigation into methods that preserve the beam’s extensive propagation properties when traversing through oceanic turbulence. Namely, we determine procedures by which oceanic turbulence resistance can be improved by altering the initial beam parameters. We proceed to discuss the SDOC distribution of the proposed beams traversing through turbulence.

Figure 4 displays the SDOC modulus of the SSS beams at propagation distance of $z = 300$ m in oceanic turbulence for various beam order values and coherence lengths. It is possible to confirm that the SDOC distribution of the SSS beams is altered by both the beam order and coherence length. The Gaussian to non-Gaussian distribution changes when the

beam order and coherence change, suggesting that SSS beams containing low coherence and higher beam order are little impacted by oceanic turbulence.

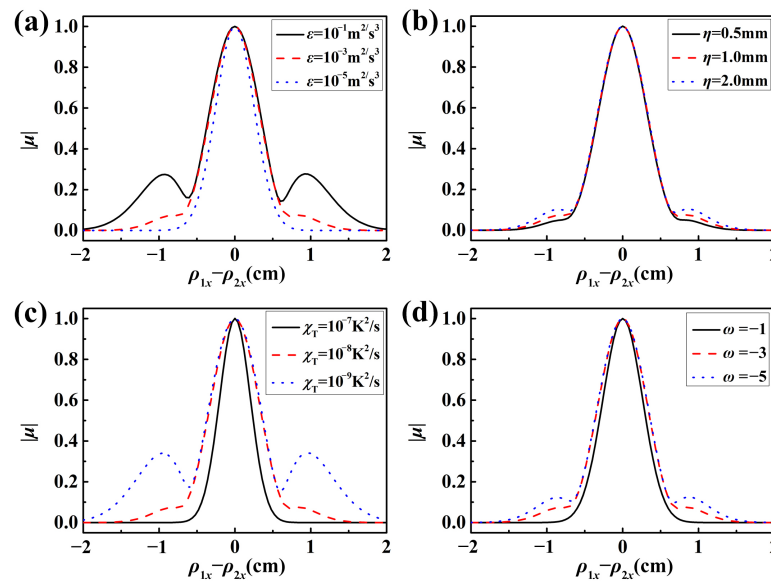


Figure 3. Cross line ($\rho_{1y} - \rho_{2y} = 0$) of the SDOC modulus at a propagation distance of $z = 300$ m for various oceanic turbulence parameters: (a) the kinetic energy dissipation rate per unit mass of the fluid; (b) the Kolmogorov inner scale; (c) the dissipation rate of the mean-square temperature; (d) the relative strength of the temperature to salinity undulations.

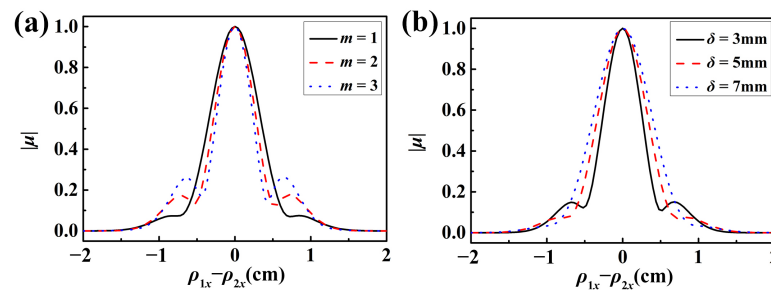


Figure 4. Cross line ($\rho_{1y} - \rho_{2y} = 0$) of the SDOC modulus at a propagation distance of $z = 300$ m for various (a) beam orders and (b) coherence lengths.

We then concentrate on the development of the spectral intensity of SSS beams traveling through ocean turbulence. Figure 5 depicts the relationship between the maximum spectral intensity within the transverse plane and the optical axis ratio for the SSS beams at propagation distance $z = 1$ km for various beginning beam characteristics. According to Figure 5a, the ratio is equal to one when the dissipation rate is very low, and it gradually declines as the dissipation rate increases. This means that when the dissipation rate is high, the beam profile remains split but, as it falls, the spots of the four beams combine to create one spot that represents a single beam. We provide new evidence that oceanic turbulence with low fluid kinetic energy dissipation rates per unit mass significantly hinders the propagation of SSS beams from the standpoint of spectral intensity deterioration. Furthermore, under the same oceanic turbulence, such ratio of the large-beam order and low-coherence SSS beams is smaller than that of the small-beam order and high-coherence SSS beams. This suggests that the SSS beams that contain a high-beam order and low coherence are more resistant to turbulence in the ocean. Likewise, we can get the same conclusion from Figure 5b–d.

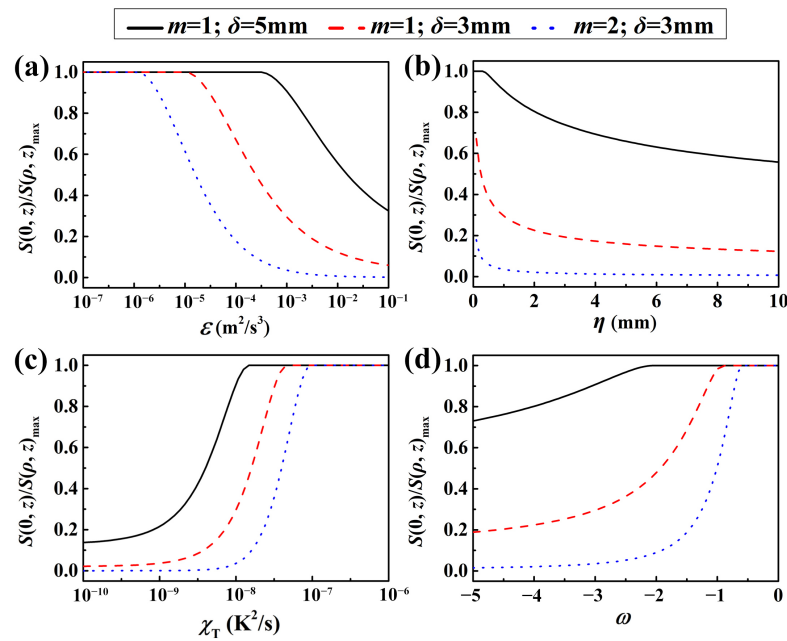


Figure 5. Ratio of the spectral intensity in the optical axis to the maximum intensity in the transverse plane of SSS beams for different beam orders and coherence lengths versus various oceanic turbulence parameters: (a) the kinetic energy dissipation rate per unit mass of the fluid; (b) the Kolmogorov inner scale; (c) the dissipation rate of the mean-square temperature; (d) the relative strength of the temperature to salinity undulations.

To more fully demonstrate the results of the coherence length or beam order on maintaining the self-splitting propagation characteristics during structured light propagation in oceanic turbulent, for various choices of beam order and coherence duration, we plot the ratio of the spectral intensity for the optical axis ($\rho = 0$) against the maximum spectral intensity in the transverse plane for the SSS beams with changing propagation distance (Figure 6). It is evident that higher-order beams with low coherence can travel further when the ratio is less than 1, that is, it exhibits improved self-splitting propagation properties, which means possessing better resistance of oceanic turbulence.

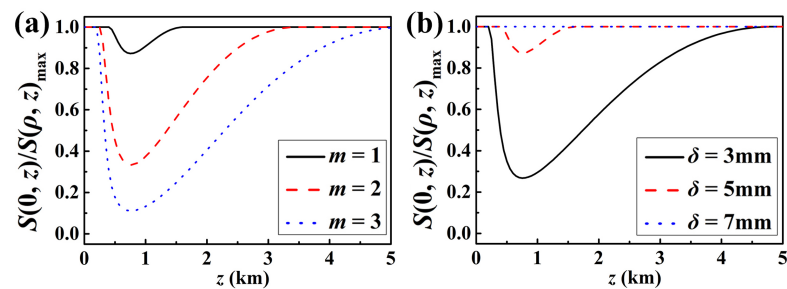


Figure 6. Ratio of the spectral intensity for the optical axis ($\rho = 0$) against the maximum intensity in the transverse plane for the SSS beams traversing through oceanic turbulence for various (a) beam orders and (b) coherence lengths.

To fully persuade readers that the SSS beam with large beam order and low coherence propose greater turbulence resistance, we search for more angles to examine the effects of beam order and coherence length on turbulence resistance. The normalized propagation factor for SSS beams traveling through oceanic turbulence for various beam orders and coherence lengths is shown in Figure 7 as it changes over time. As a control group, we also show the normalized propagation factor for Gaussian Schell-model (GSM) beam ($w = 1$ cm, $\delta = 5$ mm) under the same turbulence parameters. GSM beam is well-known and

simple partially coherent beam, and there are many studies on its propagation properties. In Ref. [31], it is confirmed that such beam can be evaluated oceanic turbulent optical wireless communication performance from the perspective of the beam wander. From Figure 7a, it can be shown that the beam order has a substantial impact on the variance of the propagation factor in turbulence. This variation grows more quickly with lower beam order, suggesting that a higher-order SSS beam is less altered by turbulence. Additionally, from Figure 7b it is determined that the coherence length has a substantial impact on the propagation factor, i.e., SSS beams containing a low coherence have reduced propagation factors. As a result, we draw the conclusion from Figure 7 that higher-order SSS beams with low coherence are less susceptible to turbulence and have superior resistance to oceanic turbulence when accounting for the propagation factor. Furthermore, we noticed that the normalized propagation factor of the GSM beam increases faster than that of the SSS beam on propagation, which means that the SSS beam modulated by the coherence structure can effectively mitigate the negative effects of turbulence.

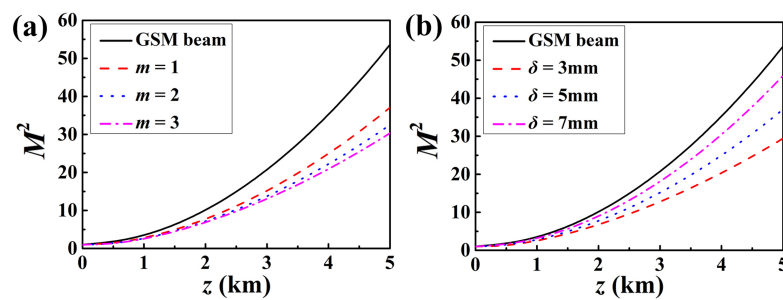


Figure 7. Normalized propagation factor for SSS beams traversing through oceanic turbulence for various (a) beam orders and (b) coherence lengths. The dark line on the graphs denotes the corresponding result for a GSM beam.

Figure 8 illustrates the relative radius of curvature for various beam orders and coherence lengths of SSS beams and GSM beam propagating in oceanic turbulence. We discover that at small propagation distances, the relative radius of curvature increases quickly, whereas at large propagation distances, it increases gradually. With the same initial beam parameters, the SSS beam has a smaller relative radius of curvature than GSM beam, furthermore, the SSS beams with large beam order and low coherence experience smaller relative radius of curvature. As a result, from the viewpoint of the relative radius of curvature, we discover once more that higher-order SSS beams with low coherence are impacted by turbulence to a lesser extent.

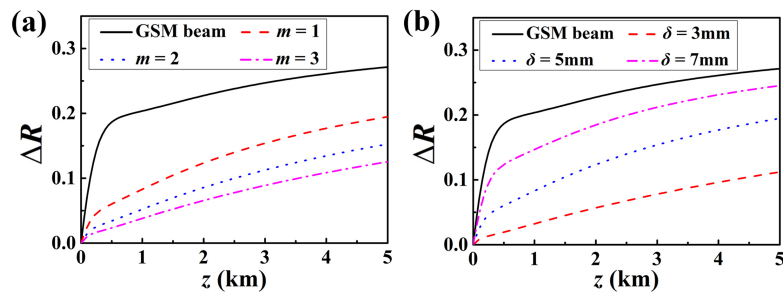


Figure 8. Relative radius of curvature of SSS beams traversing through oceanic turbulence for various (a) beam orders and (b) coherence lengths.

5. Conclusions and Discussion

We have researched how SSS beams behave statistically in the second order while they are propagating across turbulence on the ocean. From the standpoint of degenerate evolution of the SDOC and spectral intensity, it is discovered that oceanic turbulence with low kinetic energy dissipation per unit mass of the fluid and the Kolmogorov inner scale,

or strong relative temperature to salinity undulations, and the mean-square temperature dissipation rate of the turbulent ocean are likely to have a more detrimental effect on such beams. Furthermore, compared to smaller-ordered structured beams with strong coherence, larger-ordered beams with low coherence are influenced by ocean turbulence to a lesser extent.

It is important to briefly discuss the physics behind the unique statistical properties of the SSS beams and their resilience to ocean turbulence. Such beams can be viewed as a superposition of coherent Gaussian modes according to prescribed weights, and the fundamental phase elements of each coherent Gaussian modes contribute to their distinct slanted propagation. Furthermore, each mode simultaneously transverses through distinct non-interfering channels, which reduces the interference-based fluctuations and averages out turbulent fluctuations. These results could have many future application in the arena of free-space optical communication. Therefore, based on the above analysis, we can design more partially coherent light sources with other novel propagation characteristics by modifying the coherent modes and weight distributions that constitute new class of partially coherent light sources, and find the appropriate coherence modes and weight distribution that most effectively reduce the negative effects of turbulence.

Author Contributions: Writing—original draft preparation, L.L. and J.H.; writing—review and editing, J.Y. and X.Z.; conceptualization, H.C.; methodology, X.Z.; software, J.H.; data curation, Y.L.; supervision, Y.C.; project administration J.Y. and Y.C. All authors have read and agreed to the published version of the manuscript.

Funding: This research was funded by National Key Research and Development Program of China (2022YFA1404800, 2019YFA0705000); National Natural Science Foundation of China (12192254, 11974218, 12004218, 92250304); China Postdoctoral Science Foundation (2020M680093, 2022M721992); Shandong Provincial Natural Science Foundation of China (ZR2020QA067); The Open Fund of the Guangdong Provincial Key Laboratory of Optical Fiber Sensing and Communications (2020GDS-GXCG08).

Institutional Review Board Statement: Not applicable.

Informed Consent Statement: Not applicable.

Data Availability Statement: Data is contained within the article.

Conflicts of Interest: The authors declare no conflict of interest.

References

1. Andrews, L.C.; Phillips, R.L. *Laser Beam Propagation through Random Media*, 2nd ed.; SPIE: Bellingham, WA, USA, 2005.
2. Tatarski, V.I. *Wave Propagation in a Turbulent Medium*; Courier Dover Publications INC: New York, NY, USA, 2016.
3. Wang, F.; Liu, X.; Cai, Y. Propagation of partially coherent beam in turbulent atmosphere: A review. *Prog. Electromagn. Res.* **2015**, *150*, 123–143. [[CrossRef](#)]
4. Korotkova, O. Light Propagation in a Turbulent Ocean. *Prog. Opt.* **2019**, *64*, 1–43.
5. Gbur, G. Partially coherent beam propagation in atmospheric turbulence. *J. Opt. Soc. Am. A* **2014**, *31*, 2038–2045. [[CrossRef](#)] [[PubMed](#)]
6. Cai, Y.; Chen, Y.; Yu, J.; Liu, X.; Liu, L. Generation of partially coherent beams. *Prog. Opt.* **2017**, *62*, 157–223.
7. Gbur, G.; Wolf, E. Spreading of partially coherent beams in random media. *J. Opt. Soc. Am. A* **2002**, *19*, 1592–1598. [[CrossRef](#)] [[PubMed](#)]
8. Yu, J.; Chen, Y.; Liu, L.; Liu, X.; Cai, Y. Splitting and combining properties of an elegant Hermite-Gaussian correlated Schell-model beam in Kolmogorov and non-Kolmogorov turbulence. *Opt. Express* **2015**, *23*, 13467–13481. [[CrossRef](#)]
9. Shakir, S.A.; Clark, T.T.; Cargill, D.S.; Carreras, R. Far-field propagation of partially coherent laser light in random mediums. *Opt. Express* **2018**, *26*, 15609–15622. [[CrossRef](#)]
10. Yu, J.; Wang, F.; Liu, L.; Cai, Y.; Gbur, G. Propagation properties of Hermite non-uniformly correlated beams in turbulence. *Opt. Express* **2018**, *26*, 16333–16343. [[CrossRef](#)]
11. Yu, J.; Huang, Y.; Wang, F.; Liu, X.; Gbur, G.; Cai, Y. Scintillation properties of a partially coherent vector beam with vortex phase in turbulent atmosphere. *Opt. Express* **2019**, *27*, 26676–26688. [[CrossRef](#)]
12. Wang, J.; Wang, M.; Lei, S.; Tan, Z.; Wang, C.; Wang, Y. Influence of Source Parameters and Non-Kolmogorov Turbulence on Evolution Properties of Radial Phased-Locked Partially Coherent Vortex Beam Array. *Photonics* **2021**, *8*, 512. [[CrossRef](#)]

13. Sun, B.; Lü, H.; Wu, D.; Wang, F.; Cai, Y. Propagation of a Modified Complex Lorentz-Gaussian-Correlated Beam in a Marine Atmosphere. *Photonics* **2021**, *8*, 82. [[CrossRef](#)]
14. Shirai, T.; Dogariu, A.; Wolf, E. Mode analysis of spreading of partially coherent beams propagating through atmospheric turbulence. *J. Opt. Soc. Am. A* **2003**, *20*, 1094–1102. [[CrossRef](#)]
15. Gori, F.; Santarsiero, M. Devising genuine spatial correlation functions. *Opt. Lett.* **2007**, *32*, 3531–3533. [[CrossRef](#)] [[PubMed](#)]
16. Chen, Y.; Wang, F.; Cai, Y. Partially coherent light beam shaping via complex spatial coherence structure engineering. *Adv. Phys.-X* **2022**, *7*, 2009742. [[CrossRef](#)]
17. Wei, D.; Wang, K.; Xu, Y.; Du, Q.; Liu, F.; Liu, J.; Dong, Y.; Zhang, L.; Yu, J.; Cai, Y.; et al. Propagation of a Lorentz Non-Uniformly Correlated Beam in a Turbulent Ocean. *Photonics* **2023**, *10*, 49. [[CrossRef](#)]
18. Liu, Y.; Zhao, Y.; Liu, X.; Liang, C.; Liu, L.; Wang, F.; Cai, Y. Statistical characteristics of a twisted anisotropic Gaussian Schell-model beam in turbulent ocean. *Photonics* **2020**, *7*, 37. [[CrossRef](#)]
19. Lajunen, H.; Saastamoinen, T. Propagation characteristics of partially coherent beams with spatially varying correlations. *Opt. Lett.* **2011**, *36*, 4104–4106. [[CrossRef](#)]
20. Gu, Y.; Gbur, G. Scintillation of nonuniformly correlated beams in atmospheric turbulence. *Opt. Lett.* **2013**, *38*, 1395–1397. [[CrossRef](#)]
21. Chen, Y.; Ponomarenko, S.A.; Cai, Y. Experimental generation of optical coherence lattices. *Appl. Phys. Lett.* **2016**, *109*, 061107. [[CrossRef](#)]
22. Liu, Y.; Chen, Y.; Wang, F.; Cai, Y.; Liang, C.; Korotkova, O. Robust far-field imaging by spatial coherence engineering. *Opto-Electron. Adv.* **2021**, *4*, 210027. [[CrossRef](#)]
23. Thorpe, S.A. *The Turbulent Ocean*; Cambridge University: Cambridge, MA, USA, 2005; pp. 1–37.
24. Ye, F.; Xie, J.; Hong, S.; Zhang, J.; Deng, D. Propagation properties of a controllable rotating elliptical Gaussian optical coherence lattice in oceanic turbulence. *Results Phys.* **2019**, *13*, 102249. [[CrossRef](#)]
25. Liu, X.; Zhou, G.; Shen, Y. Effect of oceanic turbulence with anisotropy on the propagation of multi-sinc Schell-model beams. *Results Phys.* **2022**, *36*, 105447. [[CrossRef](#)]
26. Chen, Y.; Gu, J.; Wang, F.; Cai, Y. Self-splitting properties of a Hermite-Gaussian correlated Schell-model beam. *Phys. Rev. A* **2015**, *91*, 013823. [[CrossRef](#)]
27. Nikishov, V.V.; Nikishov, V.I. Spectrum of Turbulent Fluctuations of the Sea-Water Refraction Index. *Int. J. Fluid Mech. Res.* **2000**, *27*, 82–98. [[CrossRef](#)]
28. Dan, Y.; Zhang, B. Beam propagation factor of partially coherent flat-topped beams in a turbulent atmosphere. *Opt. Express* **2008**, *16*, 15563–15575. [[CrossRef](#)]
29. Martínez-Herrero, R.; Mejías, P.M.; Piquero, G. Quality improvement of partially coherent symmetric-intensity beams caused by quartic phase distortions. *Opt. Lett.* **1992**, *17*, 1650–1651. [[CrossRef](#)]
30. Weber, H. Propagation of higher-order intensity moments in quadratic-index media. *Opt. Quantum. Electron.* **1922**, *24*, S1027–S1049. [[CrossRef](#)]
31. Wu, Y.; Zhang, Y.; Li, Y.; Hu, Z. Beam wander of Gaussian-Schell model beams propagating through oceanic turbulence. *Opt. Commun.* **2016**, *371*, 59–66. [[CrossRef](#)]

Disclaimer/Publisher’s Note: The statements, opinions and data contained in all publications are solely those of the individual author(s) and contributor(s) and not of MDPI and/or the editor(s). MDPI and/or the editor(s) disclaim responsibility for any injury to people or property resulting from any ideas, methods, instructions or products referred to in the content.